Polymer(Korea), Vol. 39, No. 1, pp. 13-22
http://dx.doi.org/10.7317/pk.2015.39.1.13

ISSN 0379-153X(Print)
ISSN 2234-8077(Online)

캘콘기를 가지는 메타크릴레이트 고분자: 모노머 반응성비와 열적 광학적 성질

Gamze Barim†, Ozgul Altun, and Mustafa Gokhun Yayla*

Department of Chemistry, Faculty of Science and Arts, University of Adiyaman
*Physics Engineering Department, Faculty of Science and Letters, Istanbul Technical University

(2014년 2월 21일 접수, 2014년 6월 12일 수정, 2014년 7월 1일 채택)

Methacrylate Polymers Having Pendant Chalcone Moieties: Monomer Reactivity Ratios, Thermal and Optical Properties

Gamze Barim†, Ozgul Altun, and Mustafa Gokhun Yayla*

Department of Chemistry, Faculty of Science and Arts, University of Adiyaman, 02040, Adiyaman, Turkey
**Physics Engineering Department, Faculty of Science and Letters, Istanbul Technical University, 34469, Maslak, Istanbul, Turkey*

(Received February 21, 2014; Revised June 12, 2014; Accepted July 1, 2014)

Abstract: A new methacrylate copolymer that includes chalcone as a side group, poly(4-methacryloyloxyphenyl-4'-methoxystyryl ketone-*co*-styrene) was synthesized by free radical copolymerization. FTIR and ^{1}H NMR spectroscopic techniques were used to characterize the homopolymers and copolymers. The copolymerizations were carried out to high conversions. Copolymer compositions were established by ^{1}H NMR spectra analysis. The monomer reactivity ratios for copolymer system were determined by the linearized Kelen Tüdös, and Extended Kelen Tüdös methods and a non-linear least squares method. The molecular weights and polydispersity index of copolymers were measured by using the gel permeation chromatography (GPC). The effect of copolymer compositions on their thermal behavior were studied by differential scanning calorimetry and thermogravimetric analysis methods. The optical properties of the resulting copolymer were also investigated.

Keywords: copolymerization, chalcone, monomer reactivity ratio, non-linear least squares, thermal property.

Introduction

In polymer science, the polymers with a reactive functional group have been an active research area because they provide an approach to subsequent polymer modification for required applications. Functional groups give a special character to polymer structure as their properties are substantially different from the polymer chain backbone.[1-4] Recently, many researches have been carried out upon synthesis and applications of polymers that bear photosensitive groups.[5-8] The polymers that contain α, β-unsaturated carbonyl groups (also named chalcone groups) either in the backbone or in pendant position undergo a crosslinking upon irradiation with UV light. These polymers have been used as negative photoresists in printing technology,[9] macro and microlithography,[10] nonlinear optical materials,[11] holographic head-up display,[12] liquid crystals,[13] photocrosslinkable paints,[14] tissue engineering,[15] and biosensors.[16] UV radiation curing is a powerful tool in crosslinking heat sensitive polymers rapidly and modify these copolymers' physicochemical characteristics in illuminated areas.[17]

The most important feature of methacrylate type monomers is their optical clarity. Due to their high light transmittance, and good mechanical and thermal resistance, they have a fairly wide area of usage. A substantial fraction of the methacrylate products are copolymers.[18-21] Polystyrene (PSt) is one of the world's most widely used polymers. The copolymers of styrene with methacrylates are very important to industry applications such as paints, adhesives, and coatings. Even though there are many studies to determine the synthesis and reactivity rate of methacrylate copolymer that include chalcone-side chain with alkyl methacrylates in the literature[22,23] all those studies have been conducted at a low conversion. There are no reports on methacrylate copolymer containing chalcone-side chain with styrene and no high conversion investigations

†To whom correspondence should be addressed.
E-mail: gbarim@gmail.com

related to determining reactivity ratios of these systems. High conversion results are more beneficial for application because the industry always works at a high conversion ratio. Moreover, thermal stability in copolymer of methacrylate monomer including chalcone in the side-group with styrene monomer is more than the thermal stability of copolymers conducted with alkyl methacrylate.

In this study, we reported the copolymer synthesis and characterization of 4-methacryloyloxyphenyl-4'-methoxystyryl ketone (MPMSK) with styrene (St) at a high conversion. Three different methods: Kelen-Tüdös (KT),[24] Extended Kelen-Tüdös (EKT),[25] and a nonlinear least squares (NLLS)[26] were used to calculate the monomer reactivity rate. The composition drift is included within the context in the EKT and the NLLS methods and those methods are suitable for high conversion experiments. The effect of MPMSK content upon the thermal and optical properties of resulting copolymers was also investigated.

Experimental

Materials. In accordance with the usual method, 4-hydroxyphenyl-4'-methoxystyryl ketone was prepared by reacting 4-hydroxyl acetophenone with 4-methoxybenzaldehyde in ethanol at 18-20 °C.[27] Styrene (St, Aldrich) was purified by washing with 5% sodium hydroxide solution for several times, and then it was also purified by distilled water. Finally, the washed St was dried over anhydrous sodium sulfate (Na_2SO_4), and before use it was filtered and distilled under the reduced pressure. 2,2'-Azobisisobutyronitrile (AIBN) was recrystallized from chloroform-methanol mixture. The analytical grade commercial products are triethylamine, 1,4-dioxane, chloroform, tetrahydrofurane (THF) and ethanol (Merck) and those are used as received.

Synthesis of 4-Methacryloyloxyphenyl-4'-Methoxystyryl Ketone (MPMSK). The 4-methacryloyloxyphenyl-4'-methoxystyryl ketone was prepared from reaction of 4-hydroxyphenyl-4'-methoxystyryl ketone with methacryloyl chloride in the presence of triethylamine in THF at -5 to 0 °C range following the procedure of Subramanian *et al.*[27] The monomer was characterized by FTIR and ^{1}H NMR spectra as follows:

IR (cm^{-1}): 3100 and 3070 (aromatic C-H stretching), 2988 and 2848 (aliphatic C-H stretching), 1732 (C=O in ester), 1660 and 1630 (C=O in ketone), 1596 and 1510 (C=C on aromatic ring), 1245 and 1202 (**O-C**=O and **O-C**-C; respectively)

^{1}H NMR (δ ppm, $CDCl_3$): 8.08-6.96 (8H, protons on aromatic ring and 2H, -CH=CH-), 6.38 and 5.81 (CH_2=C), and 3.86 (3H, OCH_3).

Homopolymerization and Copolymerization. Homo- and copolymerization reactions were carried out in 1,4-dioxane

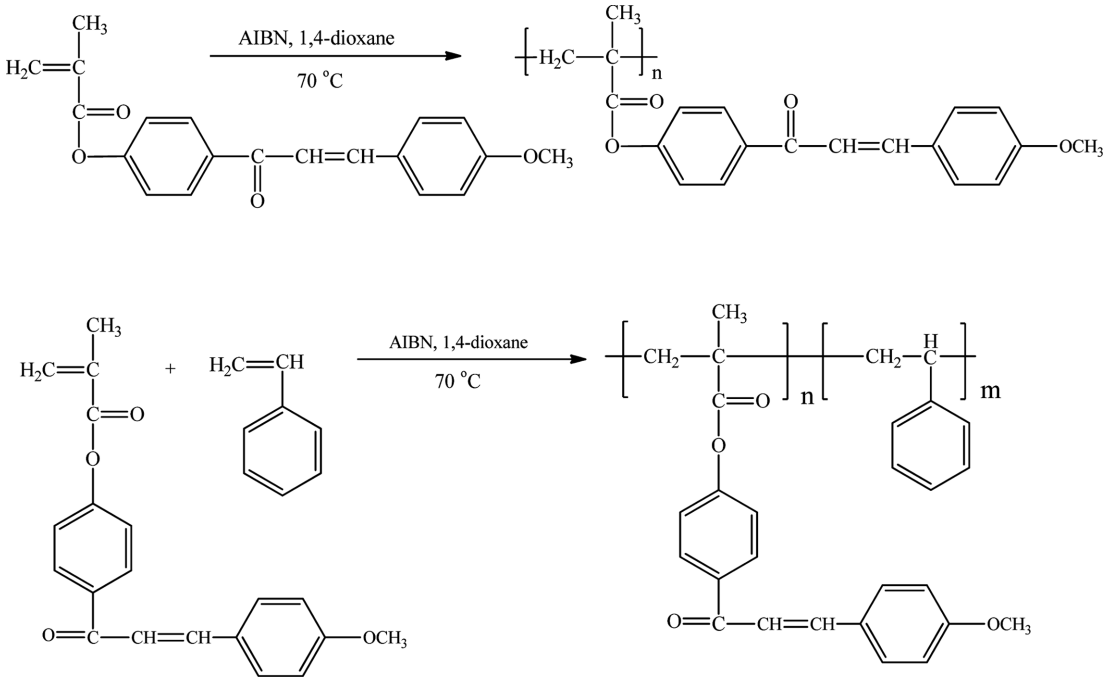

Scheme 1. Synthesis of poly(MPMSK) and poly(MPMSK-*co*-St).

Table 1. Monomer and Copolymer Composition Data, Molecular Weights and PDI Indices of Copolymers

Exp. No	Initial mon. composition		%Conversion	Final mon. composition		Copolymer composition from ^{1}H NMR		Molecular weight	
	MPMSK [A]	St [B]		MPMSK [A]_fin	St [B]_fin	MPMSK P_A	St P_B	$M_n \times 10^4$	PDI
1	0.00	1.00	-	-	-	-	-	3.2	1,64
2	0.10	0.90	16	0.08	0.76	0.22	0.78	3.5	1.70
3	0.20	0.80	20	0.16	0.64	0.36	0.64	-	-
4	0.50	0.50	26	0.37	0.37	0.50	0.50	3.6	1.74
5	0.70	0.30	31	0.48	0.21	0.55	0.45	-	-
6	0.90	0.10	42	0.52	0.06	0.80	0.20	3.9	1.91
7	1.00	0.00	-	-	-	-	-	4.2	2.03

solution at 70 ºC using AIBN (1% based on the total weight of the monomers) as the initiator by free radical copolymerization (Scheme 1, first row). The required amounts of MPMSK and St were mixed in a polymerization tube in presence of 1,4-dioxane with AIBN, and they were purged with N_2 atmosphere for 15 min. The polymerization was performed at 70 ºC in a thermostatic oil bath. After three hours, the copolymers were precipitated in excess ethanol and filtered. The precipitated polymers were purified by repeated reprecipitation and finally dried under vacuum at 40 ºC for 24 h. The conversion was determined gravimetrically. The copolymerization reaction conditions of MPMSK with St are shown in Scheme 1, second row. The copolymer compositions and conversions are given in Table 1.

The structure of the homopolymer, poly(MPMSK) was characterized by FTIR and ^{1}H NMR spectra as follows:

IR (cm^{-1}): 1751 (C=O in ester), 1662 and 1636 (C=O in ketone), 1598 and 1512 (C=C on aromatic ring), 1255 and 1210 (**O-C**=O and **O-C**-C; respectively)

^{1}H NMR (δ ppm, $CDCl_3$): 7.96-6.82 (8H, protons on aromatic ring and 2H, -CH=CH-), 3.78 (3H, OCH_3), 2.20 (-CH_2- on backbone) and 1.50 (α-CH_3)

Characterization Techniques. The infrared spectra were recorded with a Perkin Elmer spectrum one FTIR system and recorded using universal ATR sampling accessory within the wavelengths of 4000-650 cm^{-1}. ^{1}H NMR spectra of copolymers were recorded in $CDCl_3$ on a 400 MHz Bruker AVIII 400 by using tetramethylsilane as an internal reference. Gel permeation chromatography (GPC) was performed to determine the average molecular weights and polydispersity index (PDI) of all polymers. Gel permeation chromatography analysis were carried out using a high pressure liquid chromatography pump with Agilent 1100 system equipped with a vacuum degasser, a refractive index detector. The eluting solvent was tetrahydrofurane, the flow rate was 1 mL/min. Calibration was achieved with polystyrene (PSt). The glass transition temperatures resulting from the polymers were measured with Shimadzu DSC-50 thermal analyzer under nitrogen atmosphere at a 10 ºC/min heating rate. Thermal stabilities of the polymers were investigated on a Perkin Elmer TGA/DTA 7300 under N_2 flow with a heating rate of 20 ºC/min. The optical measurements of the poly(MPMSK-*co*-St) synthesized were conducted on a Shimadzu UV-*vis*-NIR3600 spectrophotometer at room temperature.

Results and Discussion

Characterization of Copolymers. The FTIR spectra of the homo and copolymers are given in Figure 1. The ester carbonyl stretching corresponds with the strong absorption band at 1745 cm^{-1}. The stronger peak at 1658 cm^{-1} and the weaker peak at 1627 cm^{-1} were attributed to the ketone carbonyl stretching. The aromatic C=C stretching is observed at 1595 cm^{-1}. The band at 1205 cm^{-1} is attributed to the C-O stretching of the ester group. The peak at 700 cm^{-1} represents aromatic C-H stretching vibration for the mono substitute benzene. Because of removal of conjugation in result of polymerization, the ester carbonyl stretching vibration in MPMSK changed from 1732 to 1745 cm^{-1} in the IR spectrum. ^{1}H NMR spectra of the homo and copolymers are given in Figure 2. The chemical shift assignments for the copolymers have been based upon the chemical shifts which have been observed for respective homopolymers. The olefinic protons of the pendant chalcone moiety and the resonance signals of aromatic protons are

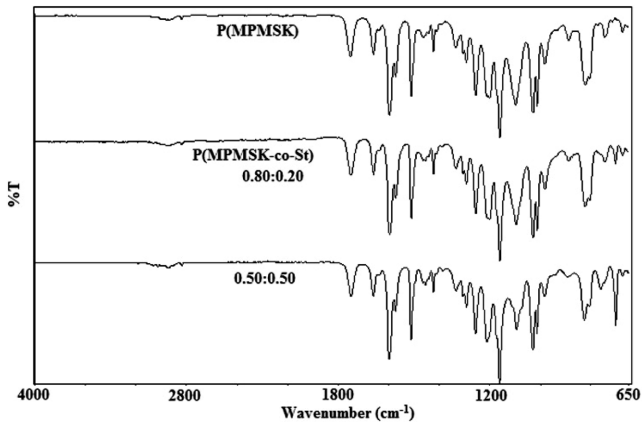

Figure 1. IR spectra of homopolymer and copolymers.

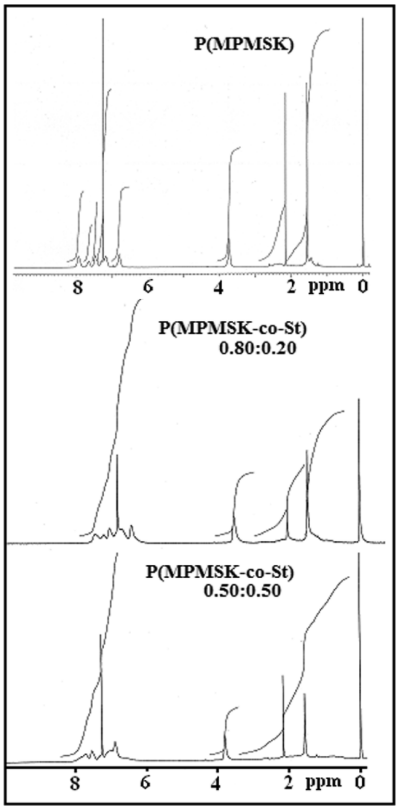

Figure 2. ^{1}H NMR spectra of homopolymer and copolymers.

between 7.90-6.90 ppm. The peak at 3.85 ppm is arisen from the OCH_3 protons of MPMSK unit. The backbone methylene protons of the two comonomer units are observed between 2.61 and 1.50. A broad signal centered at 1.28 ppm corresponds to the α-methyl protons.

Molecular weights and PDI (M_w/M_n) of the polymer samples were determined by GPC are presented in Table 1. Weight average (M_w) and number average (M_n) molecular weights of poly(MPMSK) are 8.7×10^4 and 4.2×10^4 g mol^{-1} and those of PSt are 5.2×10^4 and 3.2×10^4 g mol^{-1}, respectively. The polydispersity index of poly(MPMSK) and PSt are 2.04 and 1.64, respectively. M_w ranges from 6.0×10^4 to 7.6×10^4 g mol^{-1}, M_n ranges from 3.5×10^4 to 3.9×10^4 g mol^{-1} because different compositions of poly(MPMSK-*co*-St). The molecular weights increased with increasing percentage of MPMSK in the feed composition. The molecular weights of the monomers are 322 g mol^{-1} (MPMSK) and 104 g mol^{-1} (St); MPMSK is heavier. The higher molecular weights of the polymers with higher MPMSK content are due to this difference. PDI of the copolymers has ranged from 1.91 to 1.70. The value of PDI means that the chain termination of polymers takes place predominantly by disproportionation.[28]

Monomer Reactivity Ratio Calculations. The most common method to determine the copolymer composition is ^{1}H NMR technique.[29] Copolymer compositions determined by ^{1}H NMR are given in Table 1. The ratio of the rates of entry of the comonomers is given by the Mayo-Lewis copolymerization equation.[30]

$$\frac{d[A]}{d[B]} = \frac{[A]}{[B]}\left\{\frac{r_a[A]+[B]}{[A]+r_b[B]}\right\} \quad (1)$$

Here, [A] that represents MPMSK and [B] that represents St are the molar concentrations of the two comonomers in the feed and $d[A]/d[B]$ is the molar ratio of the two monomer entering the copolymer. The parameters r_a that represents the reactivity ratio of MPMSK and r_b that represents St are known as the monomer reactivity ratios. The composition of the copolymer depends not only on the feed composition but also on the monomer reactivity ratio. For this reason the knowledge of these ratios is essential for the manufacture of copolymers with desired properties.

Designating the initial monomer ratio by $X=[A]/[B]$ and $Y=d[A]/d[B]$ resulting copolymer ratio by and further arranging X and Y in the form of $G=X(Y-1)/Y$ and $F=X^2/Y$ and $\alpha=\sqrt{F_{min}\cdot F_{max}}$ and using $\eta=G/(\alpha+F)$ and $\xi=F/(\alpha+F)$ transformations Mayo-Lewis equation is transformed to the linearized Kelen-Tüdös version,

$$\eta = \left(r_a + \frac{r_b}{\alpha}\right)\xi - \frac{r_b}{\alpha} \quad (2)$$

The significant parameters of KT and EKT equations are presented in Tables 2 and 3. The KT plot is given as Figure 3. The KT coefficient $\alpha = 0.93$ indicates that the experimental planning was good. The data lie on the straight line with very

Table 2. KT Parameters for MPMSK-*co*-St Copolymer System

Polymer	X	Y	G	F	η	ξ
1	0.11	0.28	-0.280	0.043	-0.260	0.044
2	0.25	0.56	-0.190	0.111	-0.226	0.105
3	1.00	1.00	0.000	1.000	-0.000	0.515
4	2.33	1.22	0.420	4.454	0.170	0.825
5	9.00	4.00	6.750	20.250	0.242	0.955

α = 0.9414.

Table 3. Extended KT Parameters for MPMSK-*co*-St Copolymer System

Polymer	ξ_1	ξ_2	Z	F	G	η	ξ
1	0.352	0.138	2.90	0.033	-0.247	-0.144	0.022
2	0.360	0.160	2.56	0.085	-0.170	-0.133	0.056
3	0.260	0.260	1.00	1.000	0.000	-0.019	0.411
4	0.243	0.465	0.44	6.136	0.497	0.107	0.813
5	0.373	0.840	0.25	61.500	11.760	0.161	0.977

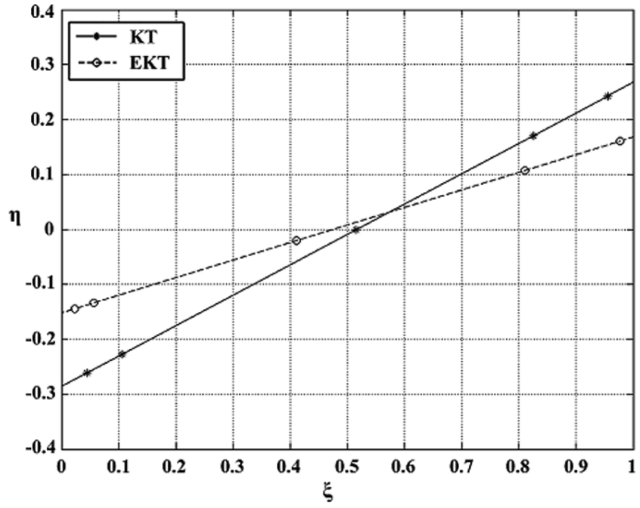

Figure 3. KT and EKT plot for MPMSK-St copolymerization.

little scatter. The reactivity ratios are found as r_a = 0.27 and r_b = 0.27.

The KT method has the advantages that the data are uniformly distributed on the so called Kelen-Tüdös plot and the results do not depend on which monomer is labeled monomer (A) and which is labeled monomer (B). Its disadvantage is that it uses the initial ratio of the two monomers rather than the reaction weighted cumulative average. When one monomer enters the reaction faster and is depleted more rapidly than the other the feed composition continuously drifts during the reaction. The KT method fails to take into account this drift. Kelen and Tüdös later proposed an extended version of their method which takes the composition drift into account.[25] Since experiments with high MPMSK fraction are stopped at 16-40% conversion; the composition drift can affect the results. For this reason the data were reanalyzed using the Extended Kelen-Tüdös (EKT) method.

EKT equation is the same as KT equation shown in eq. (2). The difference between KT and EKT methods is the calculation of F and G. In EKT method, they are calculated through $F = Y/Z^2$, $G = (Y-1)/Z$, where $Z = \log(1-\xi_1)/\log(1-\xi_2)$, and $\xi_1 = [A]_0/d[A]$, $\xi_2 = [B]_0/d[B]$ Here $[A]_0$ and $[B]_0$ are the initial molar monomer fractions.

The EKT plot is given as Figure 3. The monomer reactivity ratios are found as; r_a = 0.17 and r_b = 0.22.

In the NLLS method used, the data is fitted to a numerical solution of the Mayo-Lewis copolymerization equation. Thus errors emanating from linearization are eliminated. For each r_a, r_b pair, the copolymerization eq. (1) is integrated numerically from initial monomer concentrations to final concentration of monomer (B). The squares of the differences of the final calculated value of the monomer (A) from its experimental value

$$\Delta[A] = [A]_{\text{final\_experimental}} - [A]_{\text{final\_calculated}} \quad (3)$$

are added for each experiment and the chi-square for that set of reactivity ratios are calculated.

$$\chi^2 = \sum_{i=1}^{n} \Delta[A]_i^2/\delta A^2 \quad (4)$$

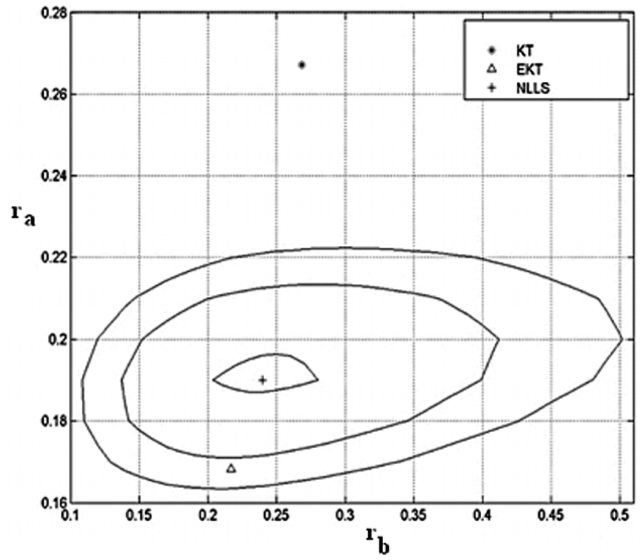

Figure 4. Probability contours and the best fit point (+) obtained by NLLS. Results of EKT (Δ) and KT(∗) are also shown on the graph.

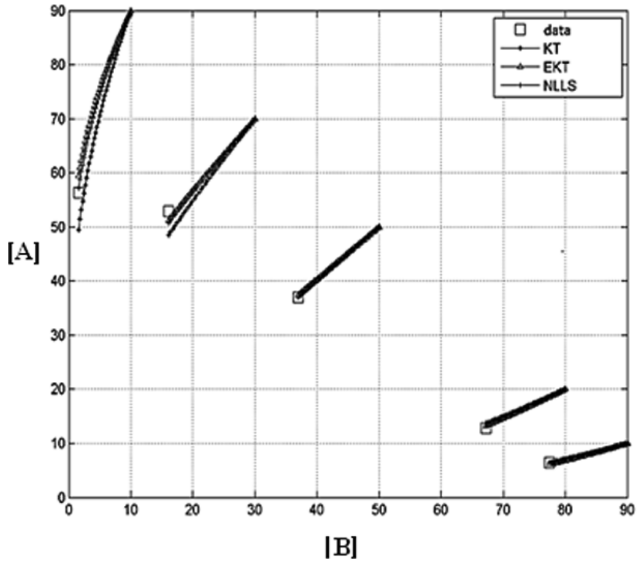

Figure 5. Evolution of the concentrations of the comonomers for all experiments. The molar concentrations are given as the percentages of the initial total molar concentration.

Here, δA is the error bar for the relevant point. The procedure is than repeated for each pair of r_a and r_b in the scanning range. The map thus produced is used for the best parameter estimate and the confidence intervals. The resulting contour map is given as Figure 4 and monomer reactivity ratios are found as; $r_a = 0.19$ and $r_b = 0.24$.

Using three different methods to evaluate the monomer reactivity ratios ensures that no algorithmic errors are present. In addition, the differences of monomer reactivity ratios calculated by the three methods give an estimate on the dependence of the results on the method of evaluation and the weighting of data points by the three methods. The EKT and NLLS results are close to each other while the KT result is somewhat outlying. Since the original KT method does not take composition drift into account and as the conversions ranged up to 40% this is expected. Figure 5 shows the numerical integration of the copolymerization equation beginning from the experimental initial conditions for each experiment using the reactivity ratios given by the three calculation techniques. The three lines starting from each initial point are the numerical integration results and the squares are the experimental data. As the reactivity ratios found by the three methods are close, the curves are similar and although results differ from experiment to experiment, overall NLLS results give the best fit.

Table 4. The Reactivity Ratios Calculated by the Three Methods

Method	KT	EKT	NLLS
r_a	0.27	0.17	0.19
r_b	0.27	0.22	0.24

a: MPMSK, b: St.

The results are summarized in Table 4. As can be seen from the table EKT and NLLS results are nearly equal with KT results slightly higher. This is due to the composition drift. Both reactivity ratios are close to 0.2 which leads to mostly alternating copolymers.

Glass Transition Temperature. The glass transition temperatures (T_g) of all the polymers were determined by differential scanning calorimeter (DSC); and DSC thermograms of polymers are given in Figure 6(a), and the T_g values are given in Table 5. Each copolymer observed has a single T_g, which indicates that it is a homogeneous phase. The T_g of poly(MPMSK) is 142 °C and T_g of PSt prepared in this work is 107 °C. The T_g of copolymers measured are between 139-117 °C. The T_g values of all the copolymers are between those of the homopolymers, shown by the dotted line in Figure 6(b). These results clearly indicate that the T_g values of the copolymers mainly depend on the composition of comonomers and the value increases with increase of molar fraction of MPMSK in the copolymer. The high T_g value of poly(MPMSK) and its copolymers can be caused by the inflexible and bulky pendant chalcone units and the short methyl chains, and this facilitate the entanglement of chain.

Thermogravimetric Analysis. For investigating the

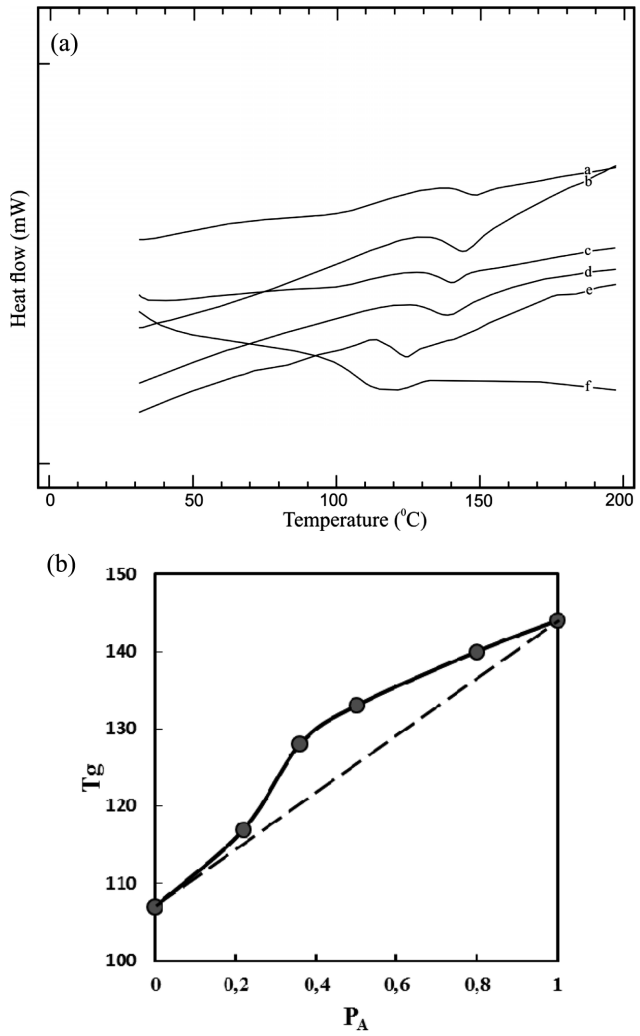

Figure 6. (a) DSC curves of investigated polymers; a: poly(MPMSK), MPMSK unit in copolymer; b: 0.80, c: 0.55, d: 0.50, e: 0.22, f: PSt; (b) Plot of glass transition temperature versus copolymer composition of poly(MPMSK-*co*-St).

decomposition characteristics of many materials, thermogravimetric analysis (TGA) has been used widely.[31,32] The TGA

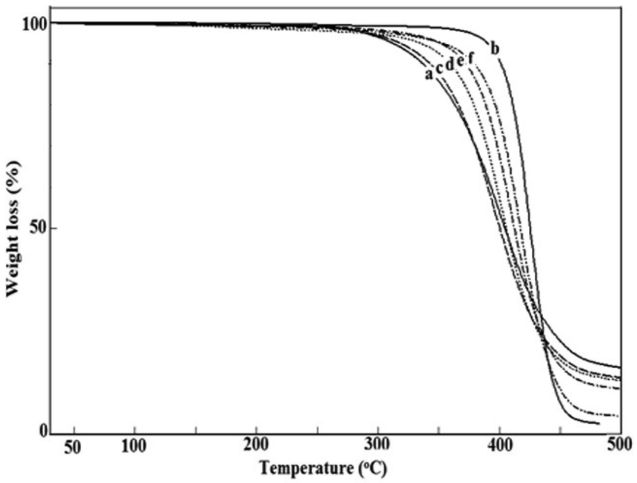

Figure 7. Thermal degradation curves of homo and copolymers; a: poly(MPMSK), b: PSt, MPMSK unit in copolymer; c: 0.80, d: 0.55, e: 0.50, f: 0.22.

curves of the homopolymer and copolymers were illustrated in Figure 7. As clearly indicated by the thermograms, all polymers subject to a single decomposition stage. The thermal behavior of a polymer should be affected appreciably by the introduction of a comonomer in the polymer chain. Therefore, it is important to analyze the thermal behavior of the copolymers. If the temperatures corresponding to 50 wt% lost of the polymers were taken as a measure for their thermal stability, these temperatures would be 412 and 422 °C for poly (MPMSK0.50-*co*-St) and poly(MPMSK0.22-*co*-St), respectively. These values are valid for those of the homopolymers which are 402 and 428 °C for poly(MPMSK) and PSt, respectively. Thermal stability of the copolymers decreased with increasing MPMSK unit. The temperatures at which weight loss begins for the MPMSK-St copolymers are somewhat lower than that of PSt. Some degradation characteristics of the copolymers were presented in comparison with the characteristics of the homopolymers in Table 5.

Table 5. Thermal Behaviour and Decomposition Temperatures of the Copolymers and Homopolymers

Polymer	T_g (°C)	% Weight loss at different temperature (°C)			
		10 (%)	30 (%)	50 (%)	70 (%)
P(MPMSK)	142	337	381	405	432
P(MPMSK 0.80)	139	343	380	400	423
P(MPMSK 0.55)	136	371	398	412	425
P(MPMSK 0.50)	133	367	408	422	433
P(MPMSK 0.22)	117	399	418	427	436
P(St)	107	401	417	427	433

The Optical Properties of the Poly(MPMSK-*co*-St). The film of the MPMSK-*co*-St synthesized coated on cleaned glasses at room temperature. The optical measurements of the MPMSK-*co*-St were measured to investigate its optical properties. The UV-vis absorption spectrum of the polymer showed two kinds of absorption bands as represented in Figure 8. The first strong absorption band is observed at 250 nm and other weak shoulder band at 390 nm. The band at 250 nm is resulted from the glass substrate. This confirmed with UV-vis spectra of bare glass substrate without coating of film. The other band at 390 nm is observed due to the π-π* transitions of >C=C< of the pendant chalcone moiety.[33]

The transmittance spectrum of the poly(MPMSK-*co*-St) is shown in Figure 9(a). As seen in Figure 9(a), the transmittance spectra of the MPMSK-*co*-St film shows a sharp absorption edge in the wavelength range about 354-442 nm. In the visible region, the average transmittance of the MPMSK-*co*-St film was found to be 83.066%. As seen in Figure 9(a), the first decrease of transmittance spectra of the poly(MPMSK-*co*-St) film starts at about 433 nm, therefore the band gap E_g of the MPMSK-*co*-St is found to be 2.864 eV. To estimate the absorption band edge of the MPMSK-*co*-St film, the first derivative of the optical transmittance can be computed. The curve of $dT/d\lambda$ *vs*. wavelength was plotted, as shown in Figure 9(b). The maximum peak value of the poly(MPMSK-*co*-St) film was found to be 432 nm. This suggests that the absorption band edge of the poly(MPMSK-*co*-St) film is 2.871 eV.

The optical band gap of optical transitions can be obtained dependence of absorption coefficient (α) on photon energy. It is evaluated that the band structure of the solution obeys the rule of direct transition and in a direct band gap material; the absorption coefficient dependence on photon energy is analyzed by,[34]

$$\alpha = A(h\nu - E_g)^m \quad (5)$$

where A is a constant, $h\nu$ is the photon energy, E_g is the optical band and m is the parameter measuring type of band gaps. To determine the optical band gap of the MPMSK-*co*-St, the $(\alpha h\nu)^{1/2}$ plot *vs*. the photon energy E of the MPMSK-*co*-St film is shown in Figure 10. As seen in Figure 10, there is a linear region for the indirect band gap of the MPMSK-*co*-St. By extrapolating the linear plot to $(\alpha h\nu)^{1/2}=0$ at the linear region, the indirect energy gap of the MPMSK-*co*-St was found to be 2.878 eV. These results suggest that the obtained indirect band gap (2.878 eV) of the MPMSK-*co*-St from the plot of $(\alpha h\nu)^{1/2}$ *vs*. E of indirect band gap of the MPMSK-*co*-St is close to obtained value (2.864 eV) of the first decrease of transmittance

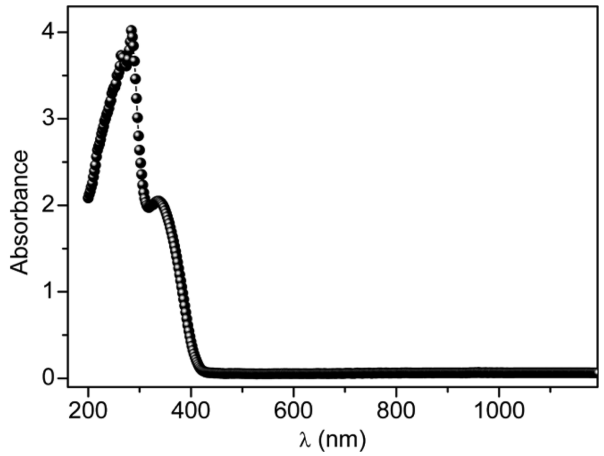

Figure 8. Absorbance of the poly(MPMSK-*co*-St) film *vs*. wavelength.

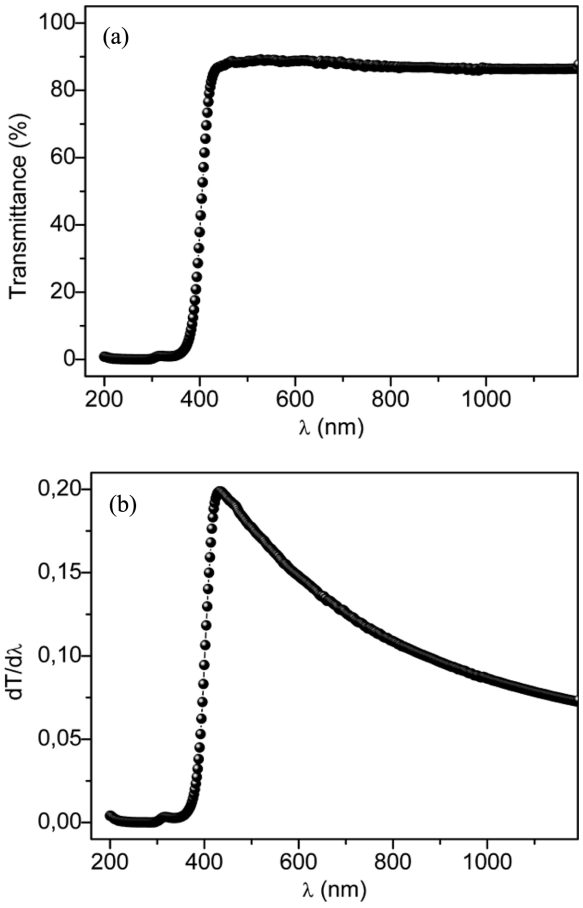

Figure 9. (a) Transmittance spectra of the poly(MPMSK-*co*-St); (b) The curve of $dT/d\lambda$ *vs*. wavelength.

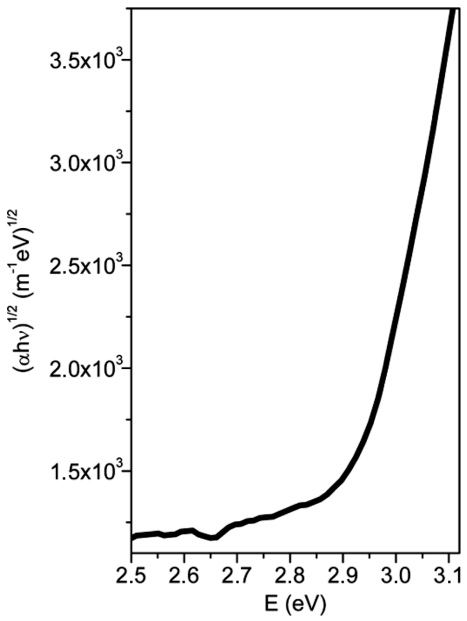

Figure 10. The $(\alpha h\nu)^{1/2}$ plot *vs.* the photon energy E of the poly(MPMSK-*co*-St) film.

spectra of the poly(MPMSK-*co*-St) and is close to value (2.871 eV) of the absorption band edge of the MPMSK-*co*-St.

Conclusions

Copolymers of MPMSK and St having different composition were synthesized by free radical polymerization in solution using AIBN as the initiator. The composition of copolymers was determined by the use of ^{1}H NMR spectra**.** The monomer reactivity ratios of the copolymers were calculated through the use of linear and nonlinear methods and the ratios were compared. As proven by the results, both reactivity ratios are less than one, close to 0.2 which leads to mostly alternating copolymers and slight composition drift. According to the DSC measurements the T_g of copolymers increased as the MPMSK content increased, as well. And, the thermal stability of the copolymers decreased as the MPMSK units in the copolymer increased. Depending on copolymer composition and thermal analysis results together it is possible to obtain copolymers with desired thermal properties. In the visible region, the average transmittance of the MPMSK-*co*-St film was found to be 83.066%. The obtained indirect band gap (2.878 eV) of the MPMSK-*co*-St from the plot of $(\alpha h\nu)^{1/2}$ *vs.* E of indirect band gap of the MPMSK-*co*-St is close to obtained value (2.864 eV) of the first decrease of transmittance spectra of the MPMSK-*co*-St and is close to value (2.871 eV) of the absorption band edge of the MPMSK-*co*-St.

Acknowledgments. The authors wish to thanks for the financial support provided by the Adiyaman University Research Fund (Project No: FBEYL 2010/0003). Also we like to thank Prof. Dr. Fahrettin Yakuphanoglu for providing the optical measurements and for his comments on the manuscript.

References

1. I. Erol, *J. Macromol. Sci. Part A: Pure Appl. Chem.*, **45**, 555 (2008).
2. K. Kwon and J-H. Chang, *Polymer(Korea)*, **38**, 232 (2014).
3. T. T. Do, Y. E. Ha, and J. H. Kim, *Polymer(Korea)*, **37**, 694 (2013).
4. C. Soykan, F. Yakuphanoglu, and M. Sahin, *J. Macromol. Sci. Part A: Pure Appl. Chem.*, **50**, 953 (2013).
5. P. Selvam, K. V. Babu, A. Penlidis, and S. Nanjundan, *Eur. Polym. J.*, **41**, 831 (2005).
6. E. C. Buruiana, F. Jitaru, N. Olaru, and T. Buruiana, *Des. Monomers Polym.*, **16**, 1 (2013).
7. R. Santhi, K. V. Babu, A. Penlidis, and S. Nanjundan, *Reac. Func. Polym.*, **66**, 1215 (2006).
8. R, Ohta, S. Ohkawa, and H. Goto, *Int. J. Polym. Mater.*, **61**, 395 (2012).
9. S. Tazuke, *Developments in Polymer Photochemistry.* Applied Science Publishers, London, UK., Vol **3** (1982).
10. H. Chen and J. Yin, *J. Polym. Sci.; Part A: Polym. Chem.*, **42**, 1735 (2004).
11. E. D. D'silva, G. K. Podagatlapalli, S. V. Rao, and S. M. Dharmaprakash, *Mater. Res. Bull.*, **47**, 3552 (2012).
12. Y. Ohe, H. Ito, N. Watanabe, and K. Ichimura *J. Appl. Polym. Sci.*, **77**, 2189 (2000).
13. G. Kumar and K. Subramanian, *J. Appl. Polym. Sci.*, **552**, 158 **(**2012).
14. G. Eisele, J. P. Fouassier, and R. Reeb, *Die Angewandte Makromolekulare Chemie*, **264**, 10 (1999).
15. G. Mapili, Y. Lu, S. Chen, and K. Roy, *J. Biomed. Mater. Res. Part B: Appl. Biomater.*, **75**, 414 (2005).
16. V. C. Tsafack, C. A. Marquette, F. Pizzolato, and L. J. Blum, *Biosens. Bioelectron.*, **15**, 125 (2000).
17. D. H. Choi, S. J. Oh, S.Y. Ban, and K. Y. Oh, *Bull. Korean Chem. Soc.*, **22**, 1207 (2001).
18. J.-S. Koo, N.-S. Kwak, and T.-S. Hwang, *Polymer(Korea)*, **36**, 564 (2012).
19. S. Mageswari and K. Subramanian, *Polym. Plast. Technol. Eng.*, **51**, 1296 (2012).
20. E.-H. Kim, B.-S. Kim, K.-S. Jung, J.-G. Kim, and H.-J. Paik, *Polymer(Korea)*, **36**, 104 (2012).
21. Y. Jo and W. Hyung, *Polymer(Korea)*, **37**, 148 (2013).
22. S. Nanjundan, R. Jayakumar, and C. S. J. Selvamalar, *J. Appl.*

Polym. Sci., **99**, 2913 (2006).
23. R. Balaji and S. Nanjundan, *J. Appl. Polym. Sci.*, **86**, 1023 (2002).
24. T. Kelen and F. Tüdös, *J. Macromol. Sci.; Part A: Pure. Appl. Chem.*, **9**, 1 (1975).
25. T. Kelen, F. Tüdös, B. Turcsanyi, and J. P. Kennedy, *J. Polym. Sci. Part A: Polym. Chem.*, **15**, 3047 (1977).
26. D. Sünbül, H. Çatalgil-Giz, W. F. Reed, and A. Giz, *Macromol. Theo. Simu.*, **13**, 162 (2004).
27. K. Subramanian, V. Krishnasamy, S. Nanjundan, and A. V. R. Reddy, *Eur. Polym. J.*, **36**, 2343 (2000).
28. S. Teramachi, A. Hasegawa, M. Akatsuka, A. Yamashita, and N. Takemoto, *Macromolecules*, **11**, 1206 (1978).
29. G. Barim, K. Demirelli, and M. Coskun, *Express Polym. Lett.*, **1**, 535 (2007).
30. F. R. Mayo and F. M. Lewis, *J. Am. Chem. Soc.*, **66,** 1594 (1944).
31. G. Barim and M. G. Yayla, *Int. J. Polym. Sci.*, **2014**, Article ID 643789 (2014).
32. G. Barim, O. Altun, and M. G. Yayla, *Des. Monomers Polym.*, **17**, 610 (2014).
33. Z. Ilter, B. F. Senkal, F. Yakuphanoglu, and M. Ahmedzade, *J. Polym. Eng.*, **28**, 535 (2008).
34. M. Fox, *Optical Properties of Solids,* Oxford Master Series in Condensed Matter Physics, Oxford University Press, Oxford, p 76 (2001).